Accepted Manuscript

Geometric modelling of heterogeneous and complex foods

Sandro M. Goñi, Emmanuel Purlis

PII: S0260-8774(09)00584-6
DOI: 10.1016/j.jfoodeng.2009.11.017
Reference: JFOE 5941

To appear in: *Journal of Food Engineering*

Received Date: 10 December 2008
Revised Date: 1 September 2009
Accepted Date: 23 November 2009

Please cite this article as: Goñi, S.M., Purlis, E., Geometric modelling of heterogeneous and complex foods, *Journal of Food Engineering* (2009), doi: 10.1016/j.jfoodeng.2009.11.017

Geometric modelling of heterogeneous and complex foods

Sandro M. Goñi*, Emmanuel Purlis

Centro de Investigación y Desarrollo en Criotecnología de Alimentos (CIDCA–CONICET La Plata), Facultad de Ciencias Exactas, UNLP, 47 y 116, La Plata (1900), Argentina

MODIAL, Facultad de Ingeniería, UNLP, 1 y 47, La Plata (1900), Argentina

Abstract

A procedure to obtain realistic geometric models of foods having different inner tissues or sub–regions is developed. The proposed methodology consists in colour segmentation of food images using a distance criterion, obtaining a reduced set of pixels representing univocally all boundaries of food sub–regions, and finally construction of the geometric model through linear interpolation. The procedure was applied to samples of different nature and complexity. The geometric models were assessed in two different ways, i.e. evaluating the performance of the image segmentation step and simulating a chilling process. The former provided an objective assessment while the later verified the usefulness of the geometric models. An optimized scenario was found between the approximation degree of the food boundaries and the computational resources involved in process simulation. Furthermore, the presented procedure can be used to perform food quality evaluation.

Keywords: Irregular shape; Image colour segmentation; Food process modelling

*Corresponding author. Phone/fax: +54 221 425 4853. E–mail address: smgoni@cidca.org.ar (S. M. Goñi)

1. Introduction

Geometric modelling can be defined as the process of creating a mathematical description of the shape of a real object, and therefore is an essential step in the mathematical modelling and simulation of food engineering processes, besides transport phenomena considerations, material properties knowledge and boundary conditions assumptions. In particular, description of the geometry is of great importance when the aim of modelling is to obtain internal profiles of temperature, concentration and/or pressure, since their gradients are involved in calculation and are certainly influenced by the geometry used in simulation. Also, when quality indexes are evaluated (e.g. browning, texture, biochemical reactions, etc.), it is often required accurate information about the internal and surface distributions of the state variables. On the other hand, geometric description is also useful for other purposes than mathematical modelling such as physical properties evaluation, i.e. surface area, volume, (apparent) density, especially when irregular shaped objects are involved (Goñi et al., 2007).

Food materials are often irregular in shape and can also present various inner regions of different composition, e.g. a piece of meat can be composed by muscle(s), fat tissue(s) and bone(s). These aspects certainly add some difficulties to mathematical modelling, so various approaches are applied to deal with these materials. Respect to the irregular geometry issue, approximating the actual object to a simple regular geometry or either a sum/composition of regular geometries is widely used (Davey and Pham, 1997). Another useful approach is to define a geometric factor (e.g. Hossain et al., 1992a, 1992b), though this method is only useful for process time prediction. In order to handle heterogeneous foods, homogeneous and average material properties are often used in the whole food.

Though such approximations have been very useful in mathematical modelling, recent advances in food engineering allow thinking in a new way of performing geometric modelling and numerical simulation of food processes, i.e. considering the actual shape and (macroscopic) composition of foods. In this way, Fito et al. (2007) recognized the need for developing new models in food process engineering incorporating information about food structure and composition (among other aspects) in order to predict the real changes in the product. On this concept, a few articles can be found in literature considering process modelling in combination with irregular shaped foods having heterogeneous composition. Gustafson et al. (1979) used a corn kernel with irregular cross–section and assumed different material properties for the germ, soft and hard endosperm for heating and cooling modelling. Califano and Zaritzky (1993, 1997) simulated cooking, freezing and thawing of beef pieces considering two–dimensional irregularly shaped geometries with different thermal properties for meat and fat regions. Ngadi et al. (1997) modelled the deep–fat frying of chicken drum considering several internal regions, i.e. muscle, bone, bone marrow and cartilage; a similar procedure was used to simulate the precooking and cooling of tuna (Zhang et al., 2002). So far, these authors performed geometric modelling by using laborious methods, mostly involving manual geometric measurements, which can be a source of additional errors in the model assessment. More recently, some researchers applied image processing techniques to construct more realistic geometric models (Goñi et al., 2007, 2008; Lespinard et al., 2009; Purlis and Salvadori, 2009; Zhang and Datta, 2006).

In summary, complex geometry is one of the most difficult issues to overcome in mathematical modelling and simulation of food processes. In this way, our ultimate objective is to develop and improve geometric modelling methods in order to be able to consider the actual geometry of the products (in terms of shape and composition) in food process simulation. Then, the specific objective of the present paper was to develop a procedure to obtain high realistic geometric models of irregular shaped foods presenting different inner tissues or regions (in a macroscopic sense). The developed approach was assessed using several samples of different complexity and also by simulating a typical food operation using the obtained geometric models.

2. Materials and methods

2.1. Samples

The developed procedure was applied to samples of different nature: beef steaks with and without bone, beef ribs, Spanish ham, Argentinean cookie (*alfajor*), sweet biscuit and *salchichón* (a kind of pork sausage). These samples were selected with the aim of covering a wide range of complexity with respect to the number of sub–regions or material composition and the distribution of such sub–regions in the food.

2.2. Image acquisition

Acquisition of food images was done using a digital colour camera (Canon PowerShot G9, Japan) due to its low cost and availability, besides that true colour images are obtained (RGB format, 3000×4000 pixels resolution). Note that other acquisition systems could be used such as computerized tomography or magnetic resonance imaging (Goñi et al., 2008), but they are expensive and less available techniques though they are not destructive. No special acquisition system was used; however, the background and illumination were selected to enhance the contrast with respect to each sample and minimize perturbations in images to ensure a successful further segmentation.

2.3. Geometric modelling

A procedure for obtaining geometric models of heterogeneous and complex foods was developed using MATLAB® (The MathWorks Inc, USA). This procedure was focused on irregularly shaped materials presenting different inner tissues or sub–regions of homogeneous composition (in macroscopic terms). The method consists in three main steps:

1. Image segmentation based on a distance criterion.
2. Representation of all boundaries of sub–regions by a reduced and univocal set of pixels.
3. Construction of a geometric model (continuous mathematical representation) of the food.

2.4. Assessment of geometric models

To verify the usefulness of the constructed geometric models regarding the final purpose of our work, a chilling process of the boneless beef steak sample was simulated. The mathematical model for beef chilling proposed by Trujillo and Pham (2006) was used for process simulation, which establishes simultaneous heat and mass transfer with convective boundary conditions (including superficial evaporation). We simulated chilling using two different geometric models: (i) obtained by the developed approach, i.e. considering both fat and meat regions; (ii) considering a unique region. In the first case, different thermophysical properties were used for each material and water diffusion was neglected in the fat region, while averaged values were used in the later. Thermophysical properties were computed according to food composition (Choi and Okos, 1986). Operating conditions were the following: heat transfer coefficient, h = 8 W m^{-2} K^{-1}; mass transfer coefficient, k_g = 5×10^{-8} kg m^{-2} s^{-1} Pa^{-1}; air temperature, 2 ºC; relative humidity, 90%. Uniform initial conditions were established for temperature and water content, 35 ºC and 75% (wet basis), respectively. Simulations were performed using the finite element method in COMSOL™ Multiphysics (COMSOL AB, Sweden).

3. Results and discussion

3.1. Image segmentation

The objective of segmentation is to separate the original image into non–overlapping regions, i.e. to assign to each pixel of the image a label corresponding to a certain sub–region previously defined, e.g. fat or meat in a piece of meat. For this aim, food images were processed according to a sequence of sub–steps (Table 1). First, depending on the quality of the original image, a filtering operation could be necessary to reduce the image noise. Next, we defined the sub–regions to be segmented from the food image, e.g. in Figure 1a, we identified two sub–regions: meat and fat–bone (for simplicity). Then, a region of interest (ROI), i.e. a representative sample of a given region or object, of each sub–region was selected. This operation consists in extracting the pixels of the image where the ROI is located. In this work, such selection was done through the function *roipoly* of MATLAB. From each ROI, average and standard deviation values were calculated to obtain representative information of the sub–regions. It is worth to note that the total number of statistic descriptors depends on the image representation; if RGB images are used, average and standard deviation values of each colour layer (R, G and B) can be obtained for each ROI.

Following, a characteristic distance of each pixel of the image to each ROI was computed by using the selected descriptors. Such a distance can be the Euclidean distance (Eq. (1)) or the Mahalanobis distance (Eq. (2)), among others (Gonzalez and Woods, 2002). Another distance can be defined by assuming a normal distribution for the RGB values of the ROI: from the *z*–value definition, a distance is calculated and used to decide if a given pixel belongs to a certain sub–region in a probabilistic way; such distance is called as standardized Euclidean distance (Eq. (3)). The selection of a characteristic distance is an empirical process since it depends on the particular case being analyzed. After this sub–step, we obtained a vector of characteristic distances of each pixel at position *i,j* to each ROI *q*.

Characteristic distances:

$$d_{i,j\to q} = \left[(A_{i,j} - I_q)^T (A_{i,j} - I_q) \right]^{1/2} \quad (1)$$

$$d_{i,j\to q} = \left[(A_{i,j} - I_q)^T \Omega_q^{-1} (A_{i,j} - I_q) \right]^{1/2} \quad (2)$$

$$d_{i,j\to q} = \left\| \frac{A_{i,j} - I_q}{S_q} \right\| \quad (3)$$

with:

$$A_{i,j} = \begin{bmatrix} R_{i,j} \\ G_{i,j} \\ B_{i,j} \end{bmatrix} \quad (4)$$

$$I_q = \begin{bmatrix} \overline{R}_q \\ \overline{G}_q \\ \overline{B}_q \end{bmatrix}, \qquad S_q = \begin{bmatrix} S_{R_q} \\ S_{G_q} \\ S_{B_q} \end{bmatrix} \tag{5}$$

where d is the characteristic distance, A is the original (or filtered) image, I_q and S_q represent the average and standard deviation of colours for the ROI q, respectively, Ω_q is the colour covariance matrix of ROI q and $\|\cdot\|$ denotes the 2–norm.

The next sub–step was the labelling, where an image B was constructed by assigning a label (e.g. 1 for meat and 2 for fat–bone in Figure 1a) to each pixel of the image A according to the location of the minimum in the distance vector associated to the pixel i,j:

$$B_{i,j} = \min_q (d_{i,j \to q}) \tag{6}$$

After the labelling operation, it is possible to obtain small objects isolated from their corresponding sub–regions, which actually are artefacts generated by the intrinsic noise of original images and segmentation. Bearing in mind that the objective was to construct macroscopic geometric models, these small objects could be eliminated since they could increase the computational cost in a further meshing stage involved in mathematical modelling and simulation. Two strategies can be adopted to perform this operation, a median filtering or a morphological operation of closing (Mery and Pedreschi, 2005). The characteristics of either the filter or the structural element respectively will depend on the particular case being analyzed.

Figure 1b shows the result of applying labelling including the elimination of small objects (by closing) over the sample shown in Figure 1a. As can be seen, the image segmentation procedure gave good results since inner regions were well partitioned and also the whole food was correctly segmented from the background.

Furthermore, each region appears as homogeneous since small objects were deleted after labelling operation.

3.2. Representation of boundary pixels

The fundamental step of the developed procedure is obtaining a reduced set of pixels representing univocally all boundaries of sub–regions of the food (called as matching). The aim of working with a reduced set of pixels was to decrease the computational cost while the univocal representation was a restriction implying that the boundary between two neighbour sub–regions must be described by the same set of pixels. If this restriction is not accomplished, defective geometric models will be constructed since holes or overlapping regions are obtained. So, the labelled (i.e. segmented) images were processed accordingly following various sub–steps (Table 1).

The first sub–step consisted in obtaining the coordinates of the pixels of all boundaries (i.e. internal and external) in the labelled image. For this aim, we used the function *contour* of MATLAB, which gives the level curves of a given function f for specific height values v. In our case, the function f was the labelled image and levels v were the assigned labels. To obtain the reduced set of the boundary pixels, the following procedure was performed, which is illustrated in Figure 2 by using the beef steak sample as example:

a. Selection of a sub–region in the labelled image (e.g. fat–bone in Figure 1b).
b. Selection of a boundary (internal or external) of this sub–region. Note that a sub–region can have more than one boundary, but in Figure 1b there is only one boundary for each sub–region.

c. Selection of a sub–set of pixels of the boundary selected in step b, ensuring that a closed region is obtained, i.e. the first and the last pixel of the sub–set must be the same.

d. Selection of a sub–region neighbouring to the sub–region with the filtered boundary obtained in step c (e.g. meat in Figure 1b).

e. Matching of the boundary pixels of the neighbour sub–region (selected in step d) to the sub–set of boundary pixels obtained in step c. If there is a fraction of the boundary pixels of the neighbour sub–region that are not common to the sub–region selected in step a, these pixels are filtered in a separate way. Then, all matched and independently filtered pixels are arranged in a unique coordinate vector.

Steps b–e were repeated until all the remaining boundaries of the sub–region selected in step a were processed. If there were sub–regions with boundaries that were still not matched, steps a–e were repeated. Steps a, b and d were done manually while steps c and e were performed automatically. It should be note that the intervention of the user in these steps did not have any influence on either the matching procedure or the final results of the entire method. Finally, a reduced set of pixels representing univocally all boundaries of the food image was obtained (Figure 2d).

3.3. Geometric modelling

The objective of geometric modelling is to create a continuous mathematical representation of an object from discrete information, i.e. pixels. In this way, the boundaries of the food sub–regions can be approximated through any type of curve, e.g. Hermite, Bézier, B–Spline. These curves are easy to construct when a single region is being approximated; however, when an object is composed by several sub–regions applying these representations is not straightforward. To overcome this situation, we used a first order interpolation through the sub–set of boundary pixels obtained by matching to approximate the actual boundaries; this is the simplest representation that can be used.

The final results of applying the developed procedure over samples are illustrated in Figure 2f and Figures 3–7. As can be seen, the developed procedure well approximated the boundaries of the different sub–regions and allowed obtaining geometric models that are in very good agreement with the actual samples, even in the more complex cases such as the Spanish ham or beef ribs, where the distribution of meat, fat and bone are very heterogeneous and complicated. In addition, it was also possible to obtain three–dimensional representations by revolution or extrusion operations from some samples. For instance, we considered the sweet cookie to have a symmetry axis and we attempted to reproduce reproduced the actual geometry by revolution from a half of the cross–section image (Figure 8a–c). On the other hand, we assumed a uniform distribution respect to shape and composition of boneless beef steak and therefore a 3D geometric model could be obtained by extrusion of the 2D model (Figure 8d).

Although a wide range of complexity was covered by the tested samples, the procedure is not universal and defective geometric models could be obtained in some situations. A limitation arises from the actual colour distribution of the food sample. If two different sub–regions (respect to composition) present similar colour, the characteristic distance from the pixels of a given sub–region to some ROI will be almost the same, and though a minimum in the characteristic distance vector is always found, the labelling will not be accurately perform. To deal with this issue, the following strategies could be implemented: (i) to increase the contrast between sub–regions by modifying the original RGB values (Mery and Pedreschi, 2005); (ii) to find a colour space where the differences between two “similar” regions are enhanced; (iii) to use other class of algorithms for segmentation of colour images (e.g. Sun and Du, 2004). On the other hand, the main advantage of the presented method is that the obtained geometric models are described only by spatial coordinates, which provides simplicity respect to reproducibility of the results. In other words, a given model can be constructed by different users with any programming language by only having the sub–set of boundary pixels describing the boundaries of food sub–regions.

3.4. Assessment of geometric models

The performance of the proposed method was evaluated in two different ways. Firstly, we attempted to establish an objective approach by assessing the image segmentation operation. In this sense, the following assumption was stated: if the segmentation is well performed, then the overall procedure will be accurate since the geometric model can be constructed as close as possible to the actual shape of the food. So, we analyzed the segmentation performance based on the method reported by Mery and Pedreschi (2005). An ideal segmentation was done for each image by visual interpretation using the software Microsoft Paint, and then the ratio between the pixels labelled by the developed and ideal procedure was computed (Table 2). In general, a very good performance was found. In the case of the beef ribs sample, the procedure showed the lowest performance: 15.42% of the fat sub–region pixels were not correctly labelled, which mostly were assigned to bone sub–region since 10.79% of exceeding pixels were detected. Considering the complexity of the evaluated samples, the labelling step presents a very acceptable global performance. So, taking into account the established assumption, the performance of the entire procedure will be also acceptable.

Secondly, we assessed the geometric models regarding the ultimate objective of modelling and simulating food processes. Specifically, the chilling of the boneless beef steak was simulated considering the actual (macroscopic) composition of the food, and we analyzed the case of using average material properties, which is one the strategies used to deal with complex materials. Figure 9 shows the results of simulation of 120 min chilling under the operating conditions described in Section 2.4. As can be seen, significant differences were obtained comparing temperature profiles, mostly for the local values. Temperature decreased faster in the case of considering the sample without different regions with homogeneous properties. These results show the usefulness of constructing detailed geometric models for process simulation. In this way, this paper will contribute to a further analysis of the influence of geometry in mathematical modelling, which should be complemented with an extensive validation through experimental data.

Finally, when numerical simulation is the final objective of geometric modelling, it is desirable to reduce the amount of information in order to decrease the computational cost. Therefore, we analyzed the relationship between the size of the sub–set of boundary points obtained after matching and the computing resources involved in a further meshing step. First, several geometric models of the boneless beef steak sample were obtained by varying the fraction of total boundary pixels. Such geometric models were reproduced in COMSOL Multiphysics and different finite element meshes were constructed (normal, coarse, and coarser mesh; COMSOL Multiphysics User's Guide). Figure 10 shows the results for three cases (of thirty); as more points are used for representing the boundaries of sub–regions, more realistic are the geometric models but denser become the corresponding meshes. Moreover, we found a potential relationship between the number of mesh elements and the fraction of total boundary points used to approximate the boundaries of the food sub–regions, which is independent of the meshing procedure in the tested range (Figure 11).

4. Conclusions

The proposed procedure allows obtaining high realistic geometric models of foods presenting different inner tissues or sub–regions with irregular shape. The presented method can be implemented by using any programming language, and the constructed geometric models can be reproduced or shared by only supplying spatial coordinates. The main limitation of the procedure is the dependence on image colour segmentation, since different sub–regions with similar colour could not be detected correctly. This is certainly an aspect for future research and improvement of the procedure.

For mathematical modelling and simulation purposes, there exists an optimized scenario between the approximation degree of the food boundaries and the computational cost. The number of mesh elements generated over the constructed geometric models increases significantly with the amount of boundary points used. So, the ultimate selection of the mesh elements resolution should be based on the major objective of the work as well as the available computing resources. Finally, the developed methodology could be used for other purposes such as food quality evaluation. If the procedure is stopped after segmentation, quality evaluation of each sub–region could be done, e.g. colour and texture image analysis, area measurements, assessment of the sub–regions number, analysis of object size distribution in each sub–region.

Acknowledgments

We thank Dr. Viviana O. Salvadori for the encouragement and comments given during the preparation of the work. Authors acknowledge Consejo Nacional de Investigaciones Científicas y Técnicas (CONICET), Agencia Nacional de Promoción Científica y Tecnológica (ANPCyT 2007–01090), and Universidad Nacional de La Plata (UNLP) from Argentina for their financial support.

References

Califano, A.N., & Zaritzky, N.E. (1993). A numerical method for simulating heat transfer in heterogeneous and irregularly shaped foodstuffs. *Journal of Food Process Engineering*, 16(3), 159–171.

Califano, A.N., & Zaritzky, N.E. (1997). Simulation of freezing or thawing heat conduction in irregular two–dimensional domains by a boundary–fitted grid method. *LWT–Lebensmittel–Wissenschaft und–Technologie*, 30(1), 70–76.

Choi, Y., & Okos, M.R. (1986). Effects of temperature and composition on the thermal properties of foods. In M. Le Maguer, P. Jelen (Eds.), *Food Engineering and Process Applications: Transport Phenomena*. Elsevier Applied Science, Amsterdam.

COMSOL AB. COMSOL *Multiphysics User's Guide*. Version: September 2005, COMSOL 3.2.

Davey, L.M., & Pham, Q.T. (1997). Predicting the dynamic product heat load and weight loss during beef chilling using a multi–region finite difference method approach. *International Journal of Refrigeration*, 20(7), 470–482.

Fito, P., LeMaguer, M., Betoret, N., & Fito, P.J. (2007). Advanced food process engineering to model real foods and process: The "SAFES" methodology. *Journal of Food Engineering*, 83(2), 173–185.

Goñi, S.M., Purlis, E., & Salvadori, V.O. (2007). Three–dimensional reconstruction of irregular foodstuffs. *Journal of Food Engineering*, 82(4), 536–547.

Goñi, S.M., Purlis, E., & Salvadori, V.O. (2008). Geometry modelling of food materials from magnetic resonance imaging. *Journal of Food Engineering*, 88(4), 561–567.

Gonzalez, R.C., & Woods, R.E. (2002). *Digital Image Processing* (2nd ed.). Prentice Hall, New Jersey.

Gustafson, R.J., Thompson, D.R., & Sokhansanj, S. (1979). Temperature and stress analysis of corn kernel – finite element analysis. *Transactions of the ASAE*, 22(4), 955–960.

Hossain, Md.M., Cleland, D.J., & Cleland, A.C. (1992a). Prediction of freezing and thawing times for foods of two–dimensional irregular shape by using a semi–analytical geometric factor. *International Journal of Refrigeration*, 15(4), 235–240.

Hossain, Md.M., Cleland, D.J., & Cleland, A.C. (1992b). Prediction of freezing and thawing times for foods of three–dimensional irregular shape by using a semi–analytical geometric factor. *International Journal of Refrigeration*, 15(4), 241–246.

León, K., Mery, D., Pedreschi, F., & León, J. (2006). Color measurement in $L^*a^*b^*$ units from RGB digital images. *Food Research International*, 39(10), 1084–1091.

Lespinard, R.A., Goñi, S.M., Salgado, P.R., & Mascheroni, R.H. (2009). Experimental determination and modelling of size variation, heat transfer and quality indexes during mushrooms blanching. *Journal of Food Engineering*, 92(1), 8–17.

Mery, D., & Pedreschi, F. (2005). Segmentation of colour food images using a robust algorithm. *Journal of Food Engineering*, 66(3), 353–360.

Ngadi, M.O., Watts, K.C., & Correia, L.R. (1997). Finite element method modelling of moisture transfer in chicken drum during deep–fat frying. *Journal of Food Engineering*, 32(1), 11–20.

Purlis, E., & Salvadori, V.O. (2007). Bread browning kinetics during baking. *Journal of Food Engineering*, 80(4), 1107–1115.

Purlis, E., & Salvadori, V.O. (2009). Bread baking as a moving boundary problem. Part 2: Model validation and numerical simulation. *Journal of Food Engineering*, 91(3), 434–442.

Sun, D.–W., & Du, C.–J. (2004). Segmentation of complex food images by stick growing and merging algorithm. *Journal of Food Engineering*, 61(1), 17–26.

Trujillo, F.J., & Pham, Q. T. (2006). A computational fluid dynamic model of the heat and moisture transfer during beef chilling. *International Journal of Refrigeration*, 29(6), 998–1009.

Zhang, J., Datta, A.K. (2006). Mathematical modeling of bread baking process. *Journal of Food Engineering*, 75(1), 78–89.

Zhang, J., Farkas, B.E., & Hale, S.A. (2002). Precooking and cooling of Skipjack tuna (*Katsuwonas pelamis*): a numerical simulation. *LWT–Lebensmittel–Wissenschaft und–Technologie*, 35(7), 607–616.

Figure captions

Figure 1. Picture of the beef steak with bone sample used to describe the procedure steps. (a) Original RGB image. (b) Segmented image after elimination of small objects; fat and bone were considered as one sub–region for simplicity in the explanation.

Figure 2. Sub–steps corresponding to the matching step. (a) All obtained boundaries pixels; blue and red symbols correspond to meat and fat–bone sub–regions, respectively. (b) Reduced sub–set of boundary pixels corresponding to the fat–bone region. (c) Meat region boundary pixels (in blue) matched to the reduced set of fat–bone boundary pixels (in red). (d) Reduced set of boundary pixels of meat region that are not neighbouring to fat–bone region (in black). (e) Original image and boundaries obtained by matching. (f) Geometric model of the sample.

Figure 3. Results of applying the procedure to Argentinean cookie sample. (a) Original image and approximate boundaries obtained by matching. (b) Geometric model.

Figure 4. Results of applying the procedure to Spanish ham sample. (a) Original image and approximate boundaries obtained by matching. (b) Geometric model.

Figure 5. Results of applying the procedure to pork sausage sample. (a) Original image and approximate boundaries obtained by matching. (b) Geometric model.

Figure 6. Results of applying the procedure to beef ribs sample. (a) Original image and approximate boundaries obtained by matching. (b) Geometric model.

Figure 7. Results of applying the procedure to boneless beef steak sample. (a) Original image and approximate boundaries obtained by matching. (b) Geometric model.

Figure 8. Results of applying the procedure to sweet cookie sample. (a) Original image. (b) Cross–section image with the approximate boundaries obtained by matching. (c) Three–dimensional geometric model obtained by revolution. (d) Three–dimensional geometric model of boneless beef steak sample (see Figure 7) obtained by extrusion.

Figure 9. Results of chilling simulation over the boneless beef steak, using the obtained geometric model with and without considering inner sub–regions. Surface plots of temperature correspond to 120 min chilling.

Figure 10. Approximating curves over the original image of boneless steak sample obtained by using different fractions of total boundary pixels (left) and the corresponding meshes generated using the coarse method (right). (a) 0.1; (b) 0.033; (c) 0.016.

Figure 11. Number of finite elements as a function of the fraction of total boundary points used to approximate the boundaries of the food. Symbols correspond to different procedures of meshing: squares for normal, triangles for coarse, circles for coarser.

Figure 1. Goñi and Purlis

a)

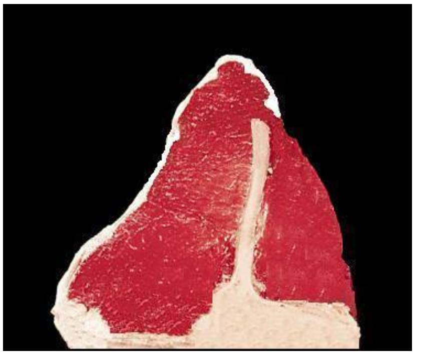

b)

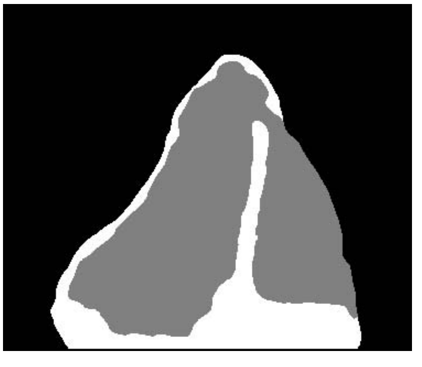

Figure 2. Goñi and Purlis

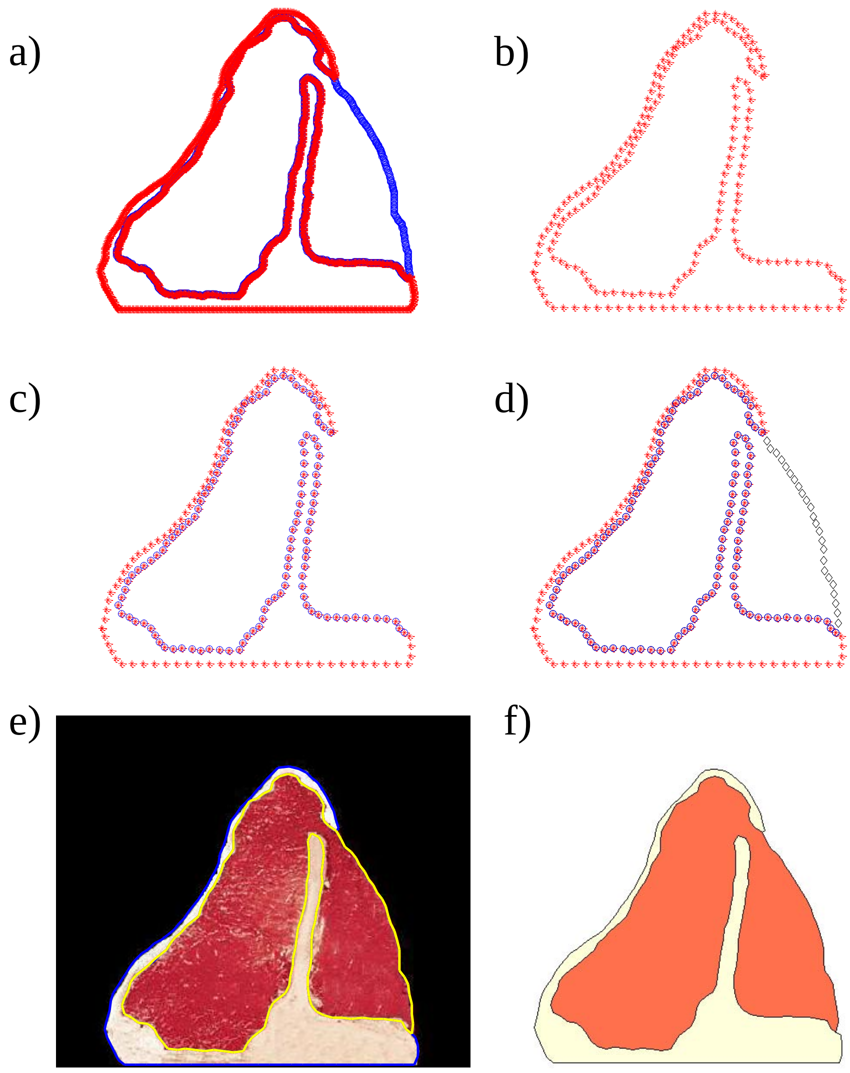

Figure 3. Goñi and Purlis

a)

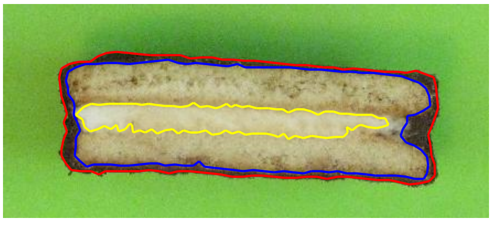

b)

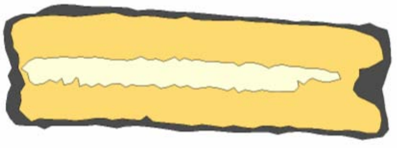

Figure 4. Goñi and Purlis

a)

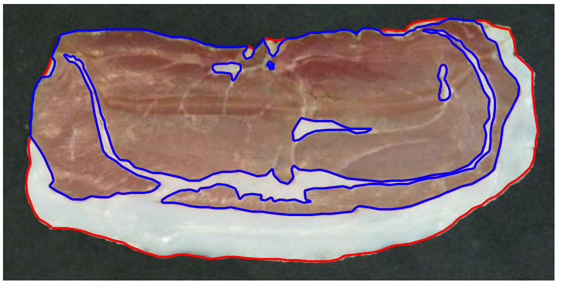

b)

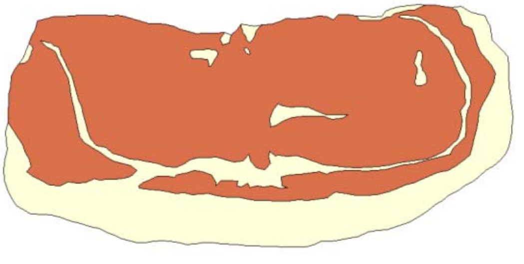

Figure 5. Goñi and Purlis

a)

b)

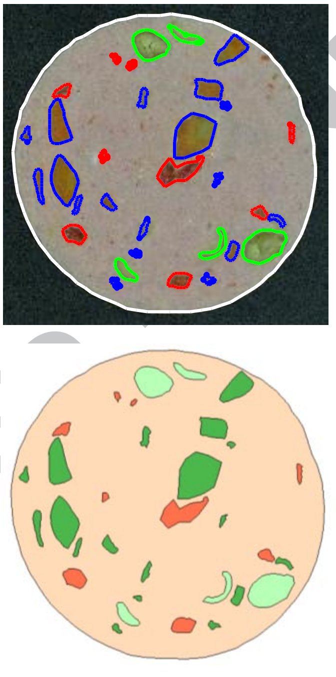

Figure 6. Goñi and Purlis

a)

b)

Figure 7. Goñi and Purlis

a)

b)

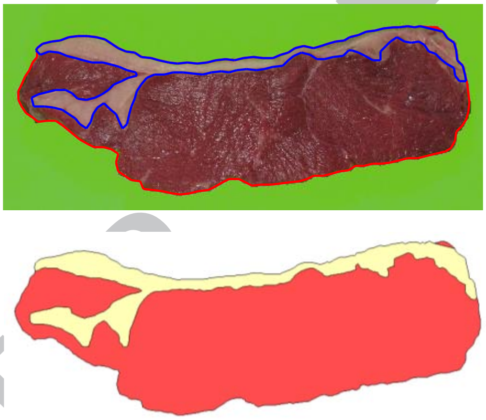

Figure 8. Goñi and Purlis

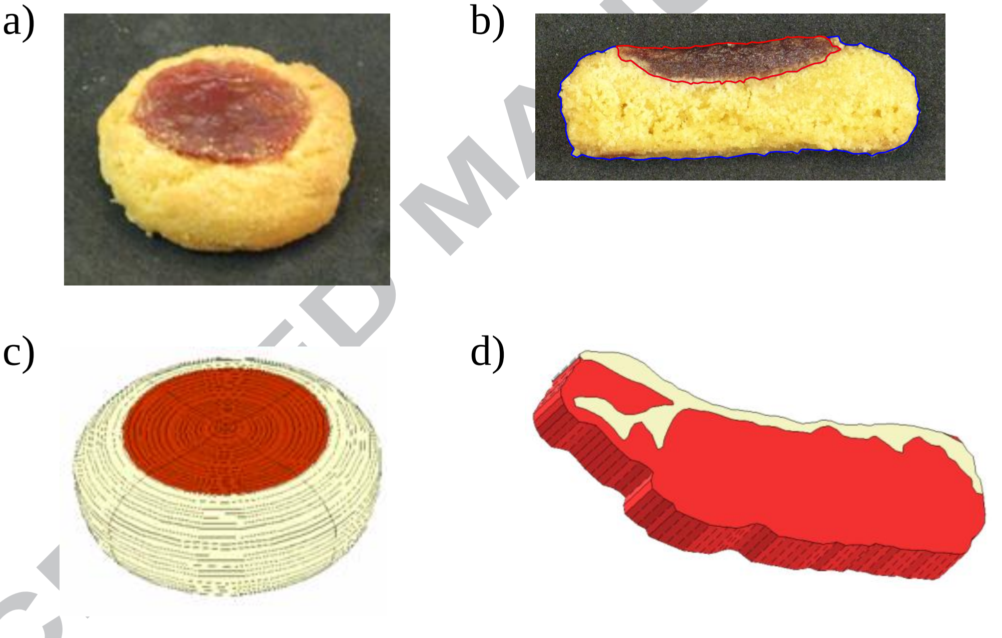

Figure 9. Goñi and Purlis

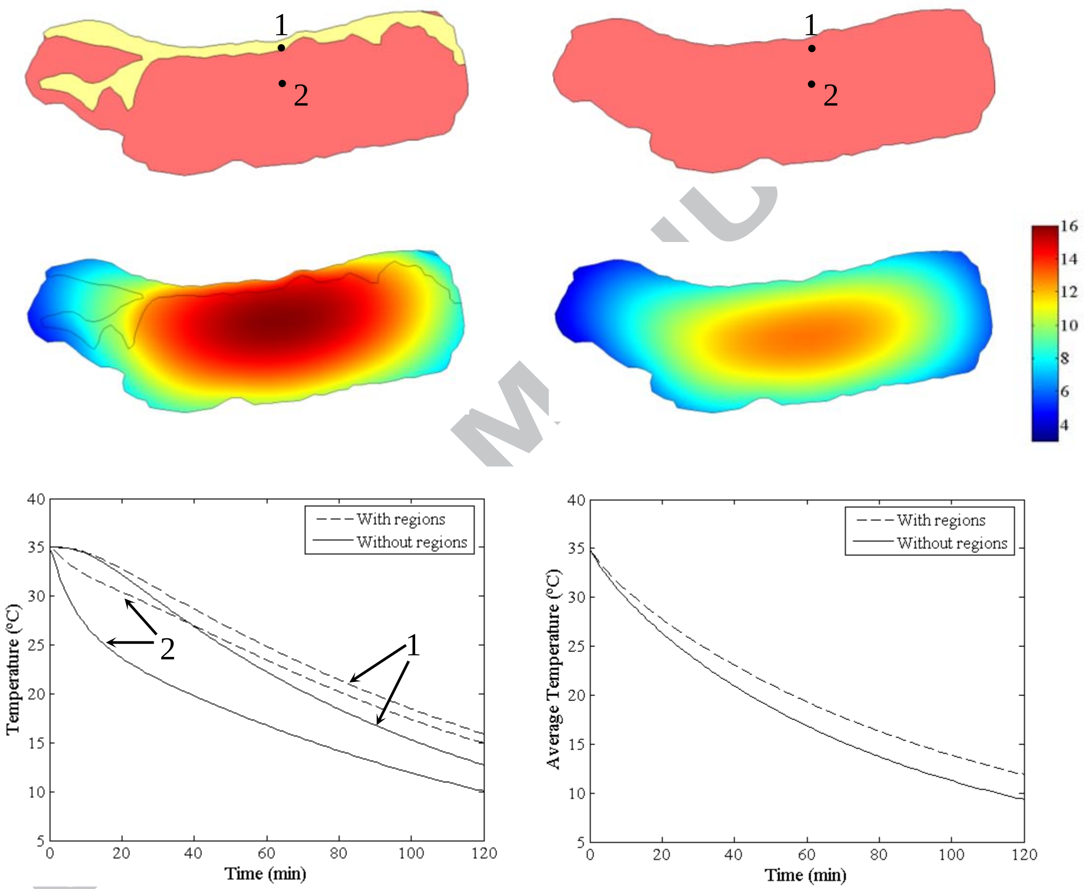

Figure 10. Goñi and Purlis

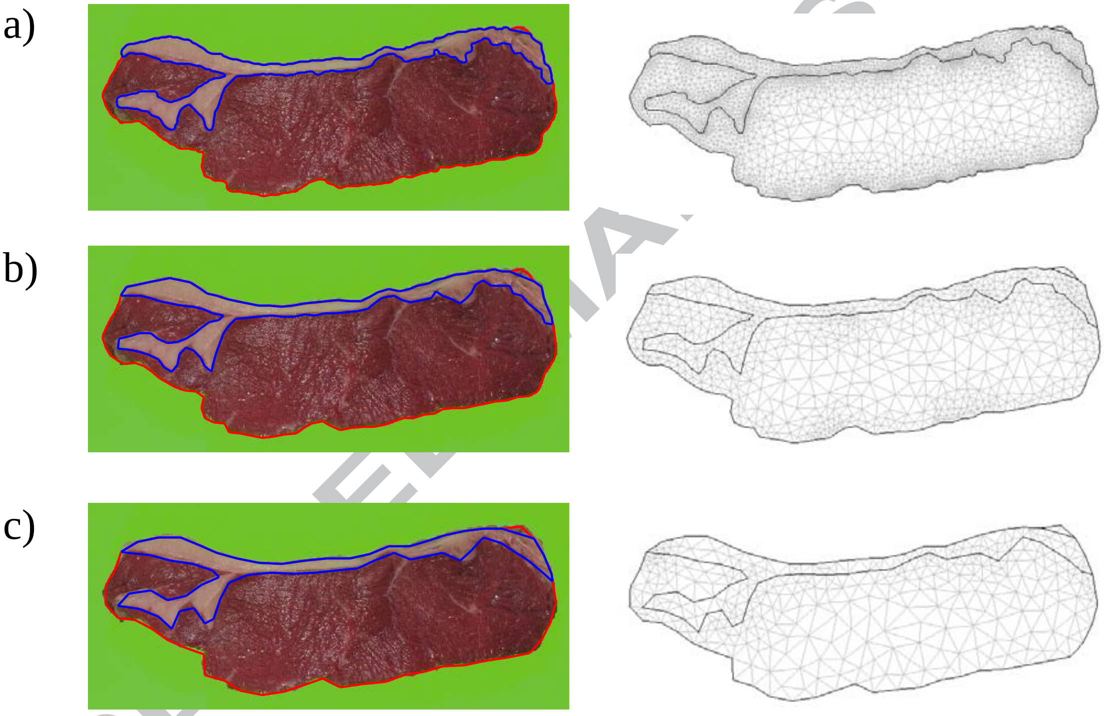

Figure 11. Goñi and Purlis

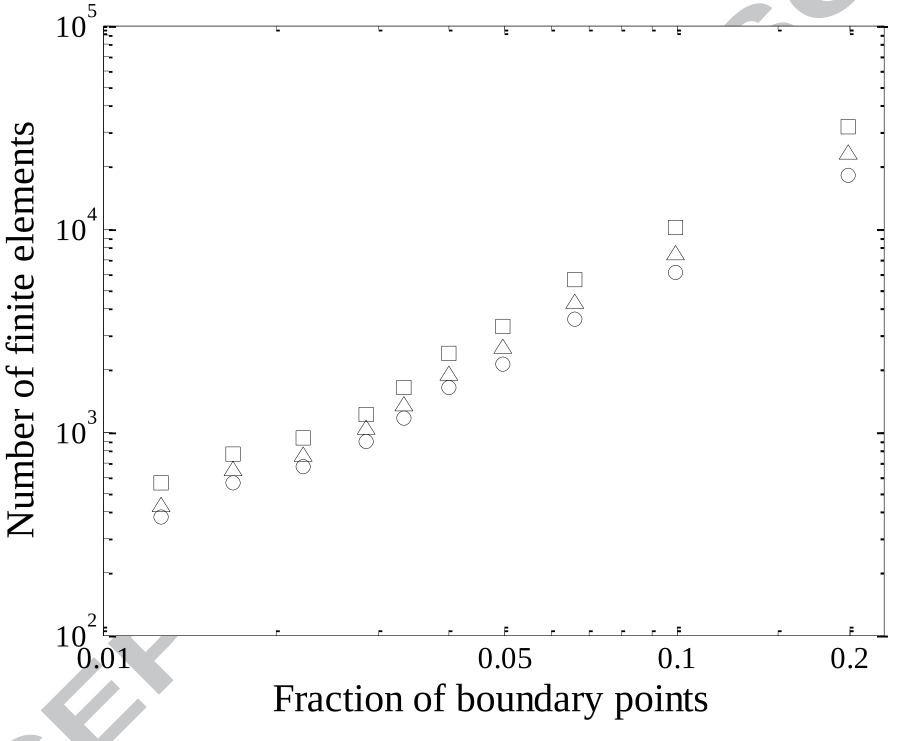

Table 1

Steps (and sub–steps) involved in geometric modelling.

Step 1. Image segmentation	
	1.1. Filtering for image noise reduction (optional)
	1.2. Selection of region of interest (ROI) for each sub–region
	1.3. Statistics on each ROI
	1.4. Calculation of the characteristic distance of each pixel to all ROI
	1.5. Pixel labelling based on minimization of pixel distance to all ROI
	1.6. Elimination of no significant or small objects (optional)
Step 2. Matching	
	2.1. Obtaining the coordinates of all boundary pixels
	2.2. Reduction of points and matching boundary pixels between different regions
Step 3. Geometric modelling	

Table 2

Performance of the segmentation step assessed by the ratio between the pixels labelled by the developed procedure and the pixels labelled by an ideal segmentation method.

Sample	Sub–region	Performance
Beef steak with bone	Fat–bone	0.9686
	Meat	0.9962
	All	0.9873
Beef steak without bone	Fat	0.9620
	Meat	0.9883
	All	0.9835
Beef ribs	Bone	1.1079
	Fat	0.8458
	Meat	1.0734
	All	1.0078
Spanish ham	Fat	0.9570
	Meat	1.0104
	All	0.9928
Argentinean cookie	Chocolate	0.8506
	Cookie	0.9019
	Filling	1.0246
	All	0.9694
Sweet biscuit	Quince jelly	0.9362
	Biscuit	1.0566
	All	1.0046
Salchichón	Olive	1.0473
	Carrot	0.9517
	Pepper	0.9684
	Meat	1.0060
	All	1.0025